Acceptance Issues for the ILC Damping Rings: Future Plans

Y. Ohnishi
KEK, Oho 1-1, Tsukuba, Japan

Damping ring is the one of key issues in the International Linear Collider(ILC). Especially, the acceptance of the damping ring is important for the delivery of the small emittance beams and sufficient bunch charges to make high luminosity operations. Dynamic aperture on the acceptance issues is studied for several lattices proposed for the ILC damping rings.

1. Estimation of Dynamic Aperture

Injection efficiency and Touschek lifetime depend on the acceptance of the accelerator ring for the injected beam or the stored beam. The acceptance should be determined by the dynamic aperture rather than the physical aperture in general. The dynamic aperture is characterized by the lattice design, especially, the sextupole magnets to correct the chromatic effects.

The dynamic aperture is evaluated by a stability for one transverse damping time. For instance, the transverse damping time of the TESLA Dogbone ring is 28 msec which corresponds to 500 turns. It is difficult to apply an analytic approach or a perturbation method because the sextupole magnets and the wiggler section cause the strong nonlinearity. Therefore, we estimate the dynamic aperture by tracking simulations numerically. In order to investigate dynamic aperture, we perform a particle-tracking simulation by using SAD[1]. SAD is an integrated code for the optics design, particle tracking, machine tuning, etc., and has been used for years at several machines such as KEKB and KEK–ATF.

Six canonical variables, x, p_x, y, p_y, z, and δ are used to describe the motion of a particle, where p_x and p_y are transverse canonical momenta which are normalized by the design momentum, p_0, and δ is the relative momentum deviation from p_0. The injected beam is a round shape in the transverse direction and coherent oscillations due to injection kickers are negligible as an assumption. Thus, we set the initial conditions as $y = x$, $p_{x0} = 0$, $p_{y0} = 0$, and $z = 0$ to evaluate the acceptance of the injected beam in these sections. We also survey a momentum aperture within ± 3 % to see a momentum aperture. As a criterion of the stability, the maximum amplitude of the particle orbit must be within 10 cm in the x and y coordinate during one damping time. Linear chromaticity is adjusted to be nearly equal 0 with optimizing the strength of the sextupole magnets for each lattice. Synchrotron radiation damping is turned on and but quantum excitation is turned off to avoid statistical fluctuations during tracking simulations.

Figure 1(a) shows the dynamic aperture of the TESLA Dogbone-S[1] obtained from the tracking simulation for the ideal lattice and the lattice includes the nonlinear wigglers described in the next section. No machine error is included in the lattice. The working point is $\nu_x/\nu_y = 72.32/47.24$. The transverse acceptance for the initial condition is expressed by $J_{y0}/J_{x0} = 1$, where $2J_{x,y}$ is the Courant-Snyder invariant and γ is the Lorentz factor. Momentum acceptance is expressed by δ_0 which is the initial momentum deviation from the design momentum. The requirement of the acceptance is assumed to be $A_x + A_y = 0.09$ m in the transverse plane and $\mid \delta_{0,max} \mid= 0.5$ % for the momentum aperture[2], where $A_{x,y}$ implies the normalized Courant-Snyder invariant, $\gamma 2J_{x,y}$.

---

[1]The lattice is modified to be a S-shape geometry and a round coupling bumps from the original TESLA Dogbone.

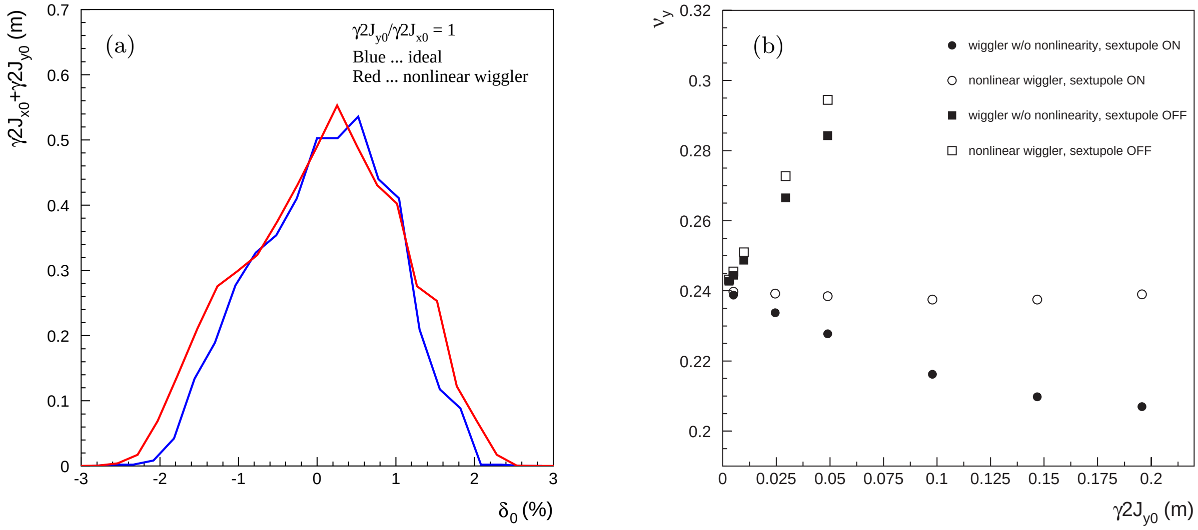

Figure 1: TESLA Dogbone-S lattice. (a) Comparison of the dynamic aperture between the ideal lattice(blue) and the lattice including nonlinear wigglers(red). The initial amplitude is set to be $J_{y0}/J_{x0} = 1$. (b) Amplitude dependence of the vertical tune. Solid circle indicates wigglers without nonlinearity and open circle indicates nonlinear wigglers with sextupole magnets turned on. Solid square indicates wigglers without nonlinearity and open square indicates nonlinear wigglers with sextupole magnets turned off.

2. Wiggler Fringe Field

A long wiggler section is necessary for the case of dogbone lattice compared with conventional designs to obtain the enough damping time while keeping the equilibrium emittance small. One of the complications implies nonlinear effects of the wiggler magnets[3].

The total Hamiltonian in the vertical plane of the ring into which wigglers are inserted can be expressed by[4]

$$H = H_0 + \frac{L_w}{4\rho_w^2} y^2 + \frac{L_w}{12\rho_w^2} k^2 y^4, \tag{1}$$

where H_0 is the Hamiltonian without the wigglers, L_w is the length of the wiggler section, ρ_w is the bending radius of the wiggler, $k = 2\pi/\lambda_w$, λ_w is the period length of the wiggler. Therefore, the associated betatron tune shift due to the wigglers is obtained from

$$\Delta\nu_y = \frac{\bar{\beta}_y}{4\pi} \left(\frac{L_w}{2\rho_w^2} + \frac{L_w}{3\rho_w^2} k^2 y^2 \right), \tag{2}$$

where $\bar{\beta}_y$ is the averaged vertical beta function in the wiggler section.

Alternatively, the Hamiltonian is parameterized by using an action variable,

$$\begin{aligned} H = 2\pi \big(&\nu_{x0} J_x + \nu_{y0} J_y + \nu_{z0} J_z + c_{xx} J_x^2 + c_{yy} J_y^2 \\ &+ c_{zz} J_z^2 + c_{xy} J_x J_y + c_{yz} J_y J_z + c_{zx} J_z J_x + \cdots \big). \end{aligned} \tag{3}$$

In the case of $J_x = J_z = 0$, the vertical betatron tune can be approximately written up to the second term as

$$\nu_y = \frac{1}{2\pi} \frac{\partial H}{\partial J_y} = \nu_{y0} + 2 c_{yy} J_y. \tag{4}$$

By comparing Eq. (2) with Eq. (4), the amplitude dependence of the vertical betatron tune due to the wigglers can be calculated by

$$c_{yy} = \frac{\bar{\beta}_y^2 L_w k^2}{12\pi\rho_w^2}. \tag{5}$$

A particle-tracking simulation by using SAD is performed to investigate the effect of the nonlinear wigglers. In SAD, the wiggler bending field is approximated by trapezoids, and the Hamiltonian up to $O(y^4)$ are included in the model. The region of the fringe field is parameterized by

$$F_1 = 6\int_{-\infty}^{+\infty}\left\{\frac{B_y(s)}{B_0} - \left(\frac{B_y(s)}{B_0}\right)^2\right\} ds, \qquad (6)$$

where B_0 is the peak field strength and $B_y(s)$ is the field component of the y-direction for the wiggler magnet. Therefore, the primary nonlinear effect of the fringe field of the wiggler magnets are included in the tracking by SAD. Figure 2 illustrates the vertical field along the wiggler axis[5] for the TESLA Dogbone damping ring and the approximated filed used in the tracking simulations. Table I shows the nonlinear coefficient, c_{yy}, estimated by the tracking for the TESLA Dogbone-S lattice without and with the nonlinear wigglers. Figure 1(b) shows amplitude dependence of the vertical tune. The nonlinear coefficient, c_{yy}, can be obtained by fitting the results from the tracking simulations shown in Table I. The difference between with and without the nonlinearity is $+2123 \sim +2203$. Using Eq. (5), the nonlinear coefficient due to the wigglers is calculated to be $+2066$ analytically, using $\bar{\beta}_y = 8.7$ m, $L_w = 417$ m, $\rho_w = 10$ m, and $\lambda_w = 0.4$ m. Consequently, the tracking simulation well reproduces the octupole-like component of the wigglers. Table I also shows the nonlinear coefficient with sextupole magnets turned on and off. The contribution of the nonlinear effects due to sextupole magnets is about -1×10^4 obtained from the sextupole magnets turned on and off. The dynamic apertures without and with the nonlinear wigglers for $J_{y0}/J_{x0} = 1$ are shown in Fig. 1(a). There is no significant difference between without and with the nonlinear wigglers.

Table I: Nonlinear coefficient c_{yy} of the damping ring estimated by the tracking simulations.

sextupoles	**w/o nonlinear wig.**	**w/ nonlinear wig.**	**deviation**
ON	-2361	-238	$+2123$
OFF	$+8858$	$+11061$	$+2203$

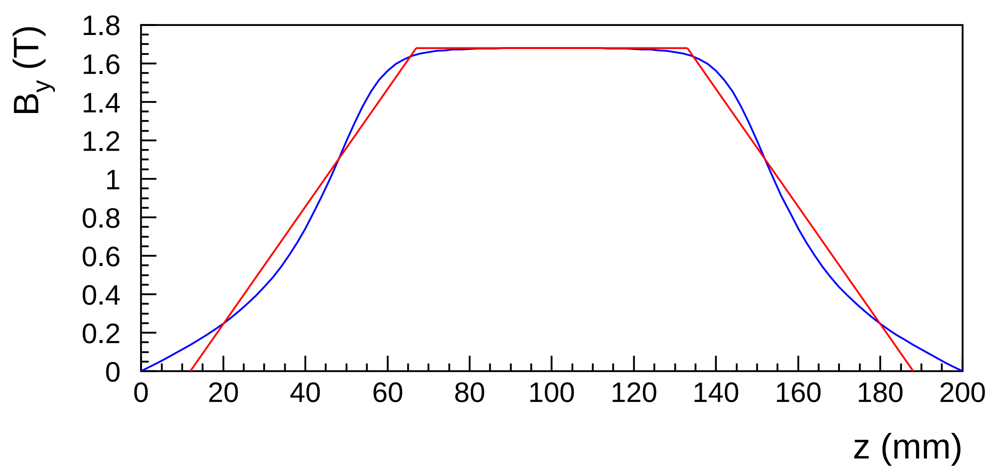

Figure 2: Wiggler field for a magnet of TESLA Dogbone damping ring. Blue line indicates a transverse vertical field along the wiggler axis and red line indicates an approximated field by a trapezoid in a tacking simulation.

3. Tune Survey of Dynamic Aperture

Figure 3 and 4 show tune surveys of the dynamic aperture described by the initial amplitude, $\gamma 2J_{x0} + \gamma 2J_{y0}$, on the tune space. The results from the ideal lattice and the lattice includes multipole errors are shown in the figure.

The multipole errors are assumed to be those based on the measurements in PEP-II and SPEAR[6]. The initial condition of the transverse acceptance is also restricted by $J_{y0}/J_{x0} = 1$. The aperture is defined by the smallest acceptance within the momentum range of ± 0.5 %. The lighter color indicates the larger dynamic aperture and the red contour shows required acceptance that corresponds to 0.09 m. The several resonances are found in the tune space. Synchro-beta resonances such as $\nu_x - \nu_s = 2N$, $3\nu_x - \nu_s = 2N$, $\nu_x + \nu_y + \nu_s = 2N$ are found in the TESLA Dogbone-S and the MCH lattice significantly. The total RF voltage is modified to be 115 MV from 54 MV to make the bunch length 7 mm in MCH lattice. However, the dynamic aperture can be kept sufficient for the injected beam for the ideal lattice and the lattice with multipole errors although dynamic apertures are decreased by 15∼20 %. The OCS lattice has a enough dynamic aperture in the large region of the tune space.

4. Results of Dynamic Aperture

The transverse aperture as a function of momentum deviation is shown in Fig. 5. Blue line indicates the ideal lattice and red line indicates the lattice that includes multipole errors. The betatron tunes are chosen so as to keep a large aperture from tune surveys shown in Fig. 3 and 4. Table II shows the results of the dynamic aperture for each lattice and the betatron tunes used in the tracking simulations. The dynamic aperture(DA) is shown by the area of acceptance in the $J_{x0} - \delta_0$ plane which is in the arbitrary unit. The effects of multipole errors are not significant in the dynamic aperture for the injected beams.

Figure 6 shows the dynamic aperture for $J_{y0}/J_{x0} = \varepsilon_y/\varepsilon_x = 0.002$ to evaluate Touschek lifetime. The emittance ratio of 0.002 is the design value including emittance tunings. The dynamic aperture is represented in the $2J_{x0}/\varepsilon_x - 2J_{z0}/\varepsilon_z$ plane. Both the ideal lattice and the lattice includes multipole errors are shown in the figure. Black line indicates the region of the dynamic aperture, $0 \leq (J_x/J_{x,max}) + (J_z/J_{z,max}) \leq 1$, to calculate probabilities of the particles lost at each component in the whole ring when the bunch is assumed to be the Gaussian distribution. Touschek lifetime for each lattice includes multipole errors is summarized in Table III. Touschek lifetime estimated by the above method is the worst case and conservative, however, the lifetime is sufficient to perform optics corrections and beam-based alignments. In order to make Touschek lifetime long, there are several ways to increase the emittance ratio with local orbit bumps at sextupole magnets or reduce number of particles per bunch.

Table II: Comparison of dynamic aperture.

	Dogbone-S	**MCH**	**OCS**	**PPA**
ν_x	72.32	75.70	50.84	47.81
ν_y	47.24	76.60	40.80	47.68
J_{y0}/J_{x0}		1		
DA(score) ideal lattice	357	296	434	319
DA(score) multipole error	344	255	428	311

Table III: Estimation of Touschek lifetime.

	Dogbone-S	**MCH**	**OCS**	**PPA**
ν_x	72.32	75.70	50.84	47.81
ν_y	47.24	76.60	40.80	47.68
$2J_{x0}/\varepsilon_x$	118	179	264	89
$2J_{z0}/\varepsilon_z$	20	14	16	14
$\varepsilon_y/\varepsilon_x$		0.002		
Number of particles/bunch		2×10^{10}		
Touschek lifetime (min)	1140	370	290	50

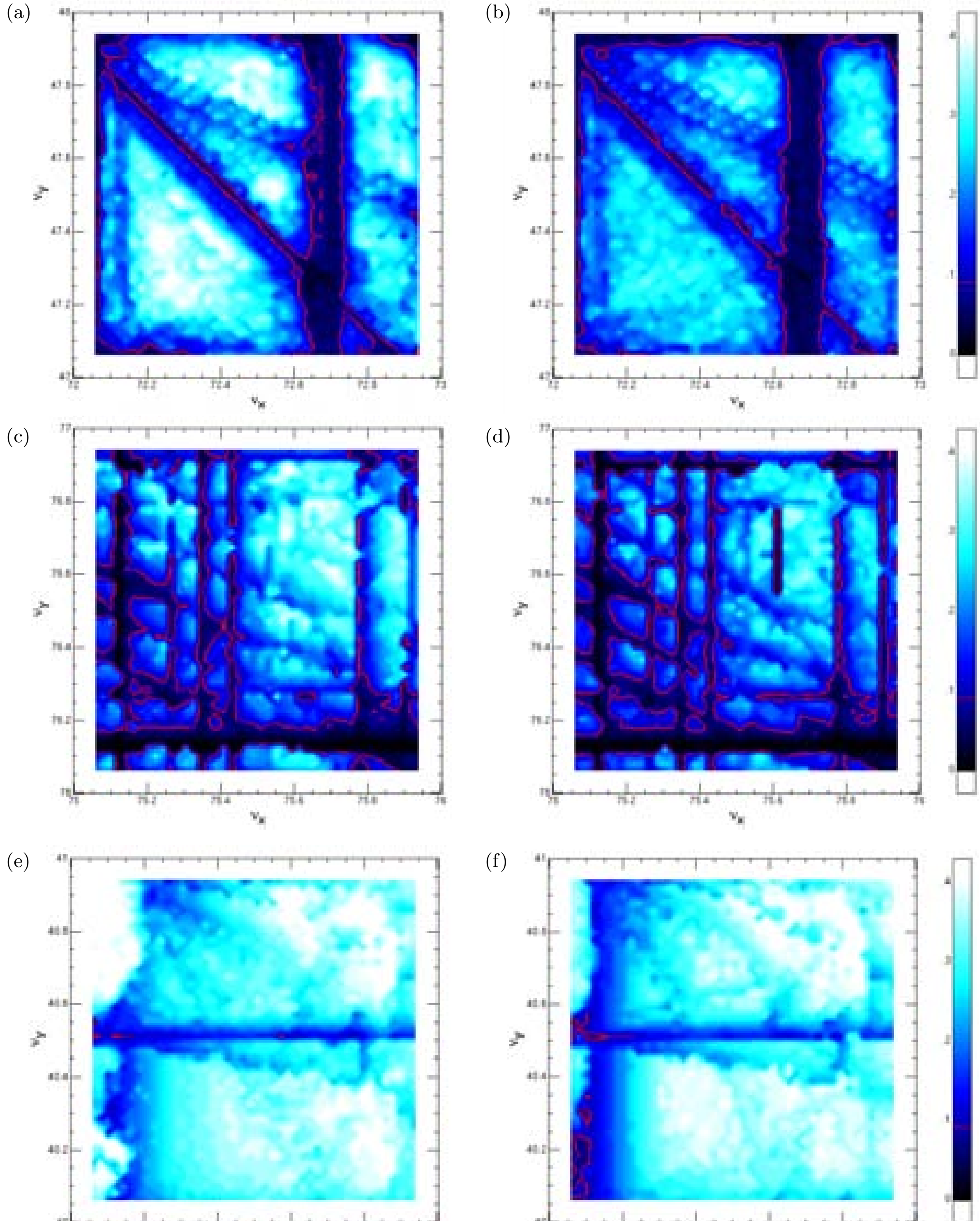

Figure 3: Tune survey of the dynamic aperture represented by the smallest $\gamma 2J_{x0} + \gamma 2J_{y0}$ for $J_{y0}/J_{x0} = 1$ within $|\ \delta_0\ | = 0.5$ %. White region shows the dynamic aperture larger than 0.4 m. Red contour indicates the requirement of the acceptance. Left: ideal lattice, (a) TESLA Dogbone-S, (c) MCH with $V_c = 115MV$, (e) OCS. Right: lattice includes multipole errors, (b) TESLA Dogbone-S, (d) MCH, (f) OCS.

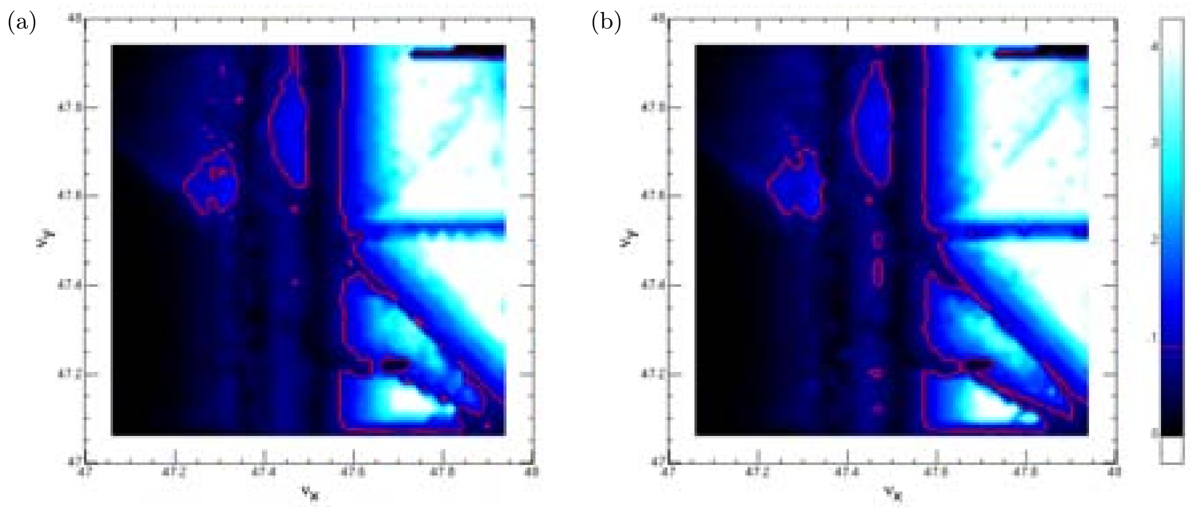

Figure 4: Same as Fig. 3. PPA, (a) ideal lattice, (b) lattice includes multipole errors.

5. Conclusion

The dynamic apertures are compared between the TESLA Dogbone-S lattice without and with the nonlinear effect of the fringe field in the wiggler magnets. The difference between them is not found significantly. The dynamic aperture obtained from the particle-tracking simulations satisfies the requirement of $A_x + A_y = 0.09$ m in the transverse plane and $| \delta_{max} |= 0.5$ % for the momentum aperture in the TESLA Dogbone-S, MCH, and OCS lattice when an appropriate working point is chosen. The acceptance requirement is still satisfied in the lattices including the multipole errors. The issue of the dynamic aperture does not restrict the choice of the circumference among 17 km, 16 km, 6 km, and 3 km .

6. Future Plans

Dynamic aperture should be studied the lattice includes the machine errors such as field gradient errors and the misalignments of the magnets cause the β-function beat, dispersion, and x-y coupling, closed orbit distortions. It is also necessary for the consideration of the nonlinear effect due to wigglers to fix the wiggler model and specifications first.

References

[1] K. Oide, Nucl. Inst. Meth. A 276, 427 (1989). http://acc-physics.kek.jp/SAD/sad.html.

[2] W. Gai, "Simulated distribution of injected positrons", http://www.desy.de/ awolski/ILCDR/DRConfigurationStudy_files/Task1.htm.

[3] D. Sagan *et al.*, " A Magnetic Field Model for Wigglers and Undulators", ICFA Beam Dyn. Newslett. 31:48-52, 2003

[4] J. Gao, "Analytical Estimation of Dynamic Apertures Limited by the Wigglers in Storage Rings", Proceedings of PAC03, p. 3267.

[5] M. Tischer, J. Pfluger, and W. Decking, "A Permanent Magnet Wiggler Design for the TESLA Damping Ring", TESLA 2000-20, December 2000.

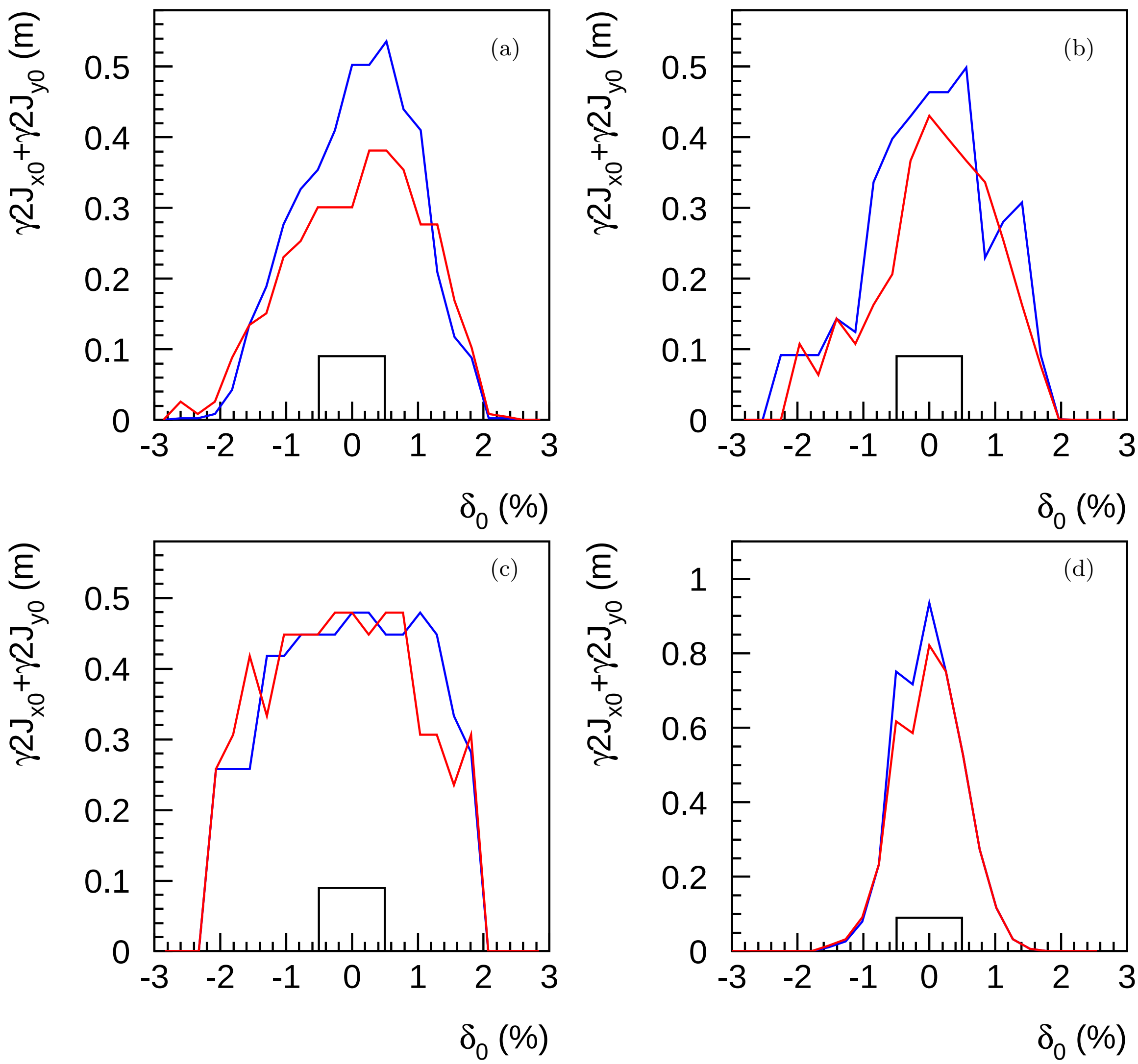

Figure 5: Dynamic aperture for $J_{y0}/J_{x0} = 1$. (a) TESLA Dogbone-S, (b) MCH with $V_c = 115$ MV, (c) OCS, (d) PPA. Blue line indicates the ideal lattice and red line indicates the lattice with multipole errors. The requirement of aperture is shown by a rectangle.

[6] Y. Cai, "Description of multipole errors used in acceptance simulations", http://www.desy.de/ awolski/ILCDR/DRConfigurationStudy_files/Task1.htm.

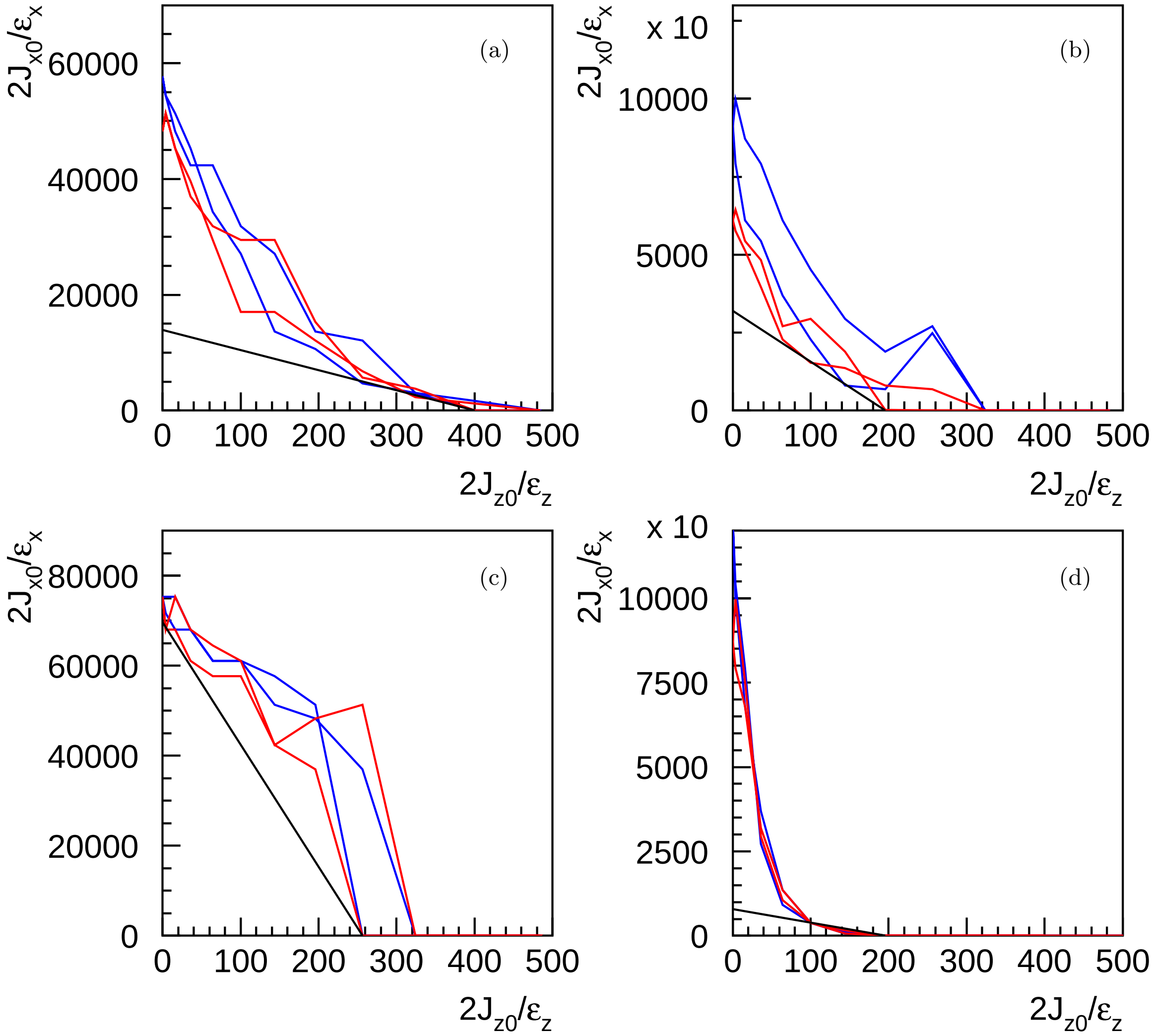

Figure 6: Dynamic aperture for $J_{y0}/J_{x0} = \varepsilon_y/\varepsilon_x = 0.002$. (a) TESLA Dogbone-S, (b) MCH with $V_c = 115$ MV, (c) OCS, (d) PPA. Blue line indicates the ideal lattice and red line indicates the lattice with multipole errors.